Implementation, Optimization, and Science Tests of Photolysis (and Chemistry) in CAM5:
(a) Uncertainty in O_3 chemistry (O_2 cross sections) propagates into climate variability
(b) Cloud-J opens capability for aerosol-cloud-chemistry interactions in climate feedbacks

Michael Prather, Juno Hsu, Alex Nicolau, Alex Veidenbaum (UC Irvine),Philip Cameron-Smith, Dan Bergmann (LLNL)

Uncertainty in the O_2 cross sections in Hertzberg Continuum (200-240 nm) is ±30% at the 90%-confidence range. The impact of this uncertainty on stratospheric climate was studied with CESM CAM5 into which Fast-J (photolysis) and Linoz (stratospheric ozone chemistry) from UC Irvine were combined with the Superfast (tropospheric) Chemistry from LLNL as part of the SciDAC research supported by the Office of Science (BER) (contracts DE-AC52-07NA27344, DE-AC02-05CH11231, DE-SC0007021). Numerical simulations were carried out using resources of the National Energy Research Scientific Computing Center (NERSC) at LLNL.

A reduction of 30% in the cross section allows more UV penetration to the lower stratosphere: increasing O_3 by 25% or more in the tropics; thereby increasing the temperatures by 1.5°K (**Fig. A1**). These changes dramatically alter O_3 in the lower stratosphere and also the temperature, but the key question asked here is whether this also alters the overall Brewer-Dobson Circulation (BDC) circulation and the net flux of stratospheric O_3 into the troposphere. We find that reducing the O_2 cross sections counterintuitively results in increased O_3 in the lowermost stratosphere (less shielding of sunlight from above), increased temperatures by up to 2°C, and thus greater static stability or stratification near the tropopause (**Fig. A2**), resulting in a lowering of the tropopause (**Fig. A3**). As a consequence, the dynamical coupling between stratosphere and troposphere changes, affecting the annual cycle as well as interannual variability, particularly in the winter (**Fig A4**), but the BD circulation of the middle stratosphere is hardly altered. We also found that this warming in the lower-middle stratosphere through increased O_3 production resulted in weakened subtropical jets and the Hadley cell (as noted by others for similar temperature perturbations associated with the solar cycle), thus indicating that photochemical uncertainties have impact on tropospheric climate as well.
Sensitivity of Stratospheric Dynamics to O_3 Production (2013), Hsu, Prather, Bergmann, Cameron-Smith, *J. Geophys. Res. Atmos.*, **118**: 8984–8999

The impact of uncertainties in O_3 chemistry on the climate are:

1. Large-scale temperature changes occur with opposite phases between the middle-upper and lower stratosphere in response to the change in ozone heating from the equator to midlatitudes. The maximum warming is 2°K.

2. Warming in the lowermost stratosphere changes the stratification of the atmosphere by increasing N^2 at the tropopause and decreasing N^2 in the stratosphere. The change in N^2 near the tropopause impedes the upward propagation of waves between 60°S and 60°N.

3. Tropopause is lowered by about 100–200 m from radiative heating of ozone, consistent with the study of Thuburn and Craig [2000, *J. Atmos. Sci., 57, 1728*].

4. Interannual variability of winter stratosphere increases in both hemispheres. However, the magnitude of the increase as well as the shift, is not nearly as large in the longer simulation of Mozart-O2jr.

5. Subtropical jets and the Hadley cell are weakened in the simulations with reduced O_2 cross sections.

6. Perturbing CAM5 MOZART and CAM4 Superfast models with the same forcing in O_3 photochemistry does not produce the same responses in secondary quantities (e.g., mean polar temperatures or seasonal cycles). s.

7. The mean Brewer-Dobson Circulation does not change in response to these large O_3-heating changes but remains tied to the overall wave forcing.
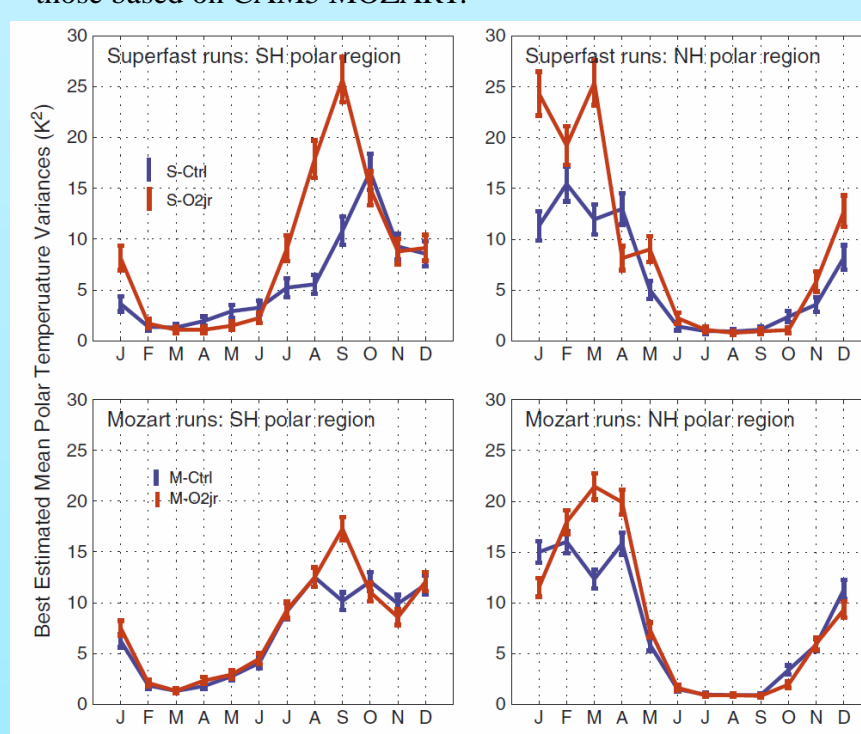
Fig. A1 Annual zonal mean changes in O3 (%) and temperature (°K) when O2 cross-sections are reduced by 30% (MOZ-r).
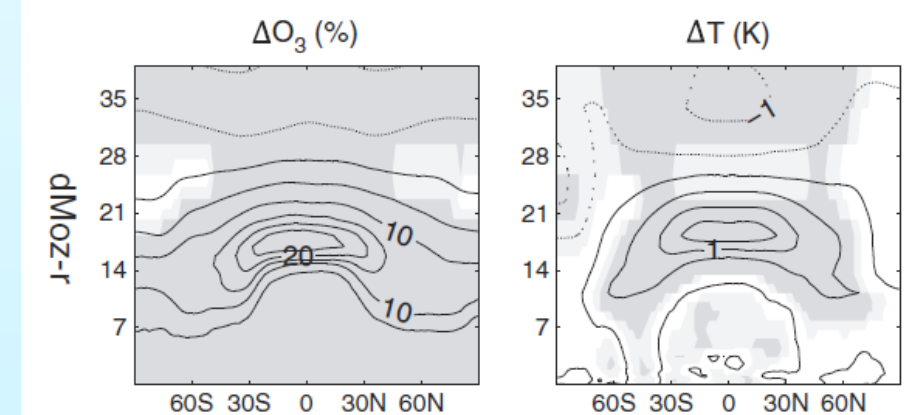
Fig. A2. Annual zonal mean changes in buoyancy (N^2) when O_2 cross-sections are reduced by 30% for both CAM4-Sfast and CAM5-MOZ(ART).
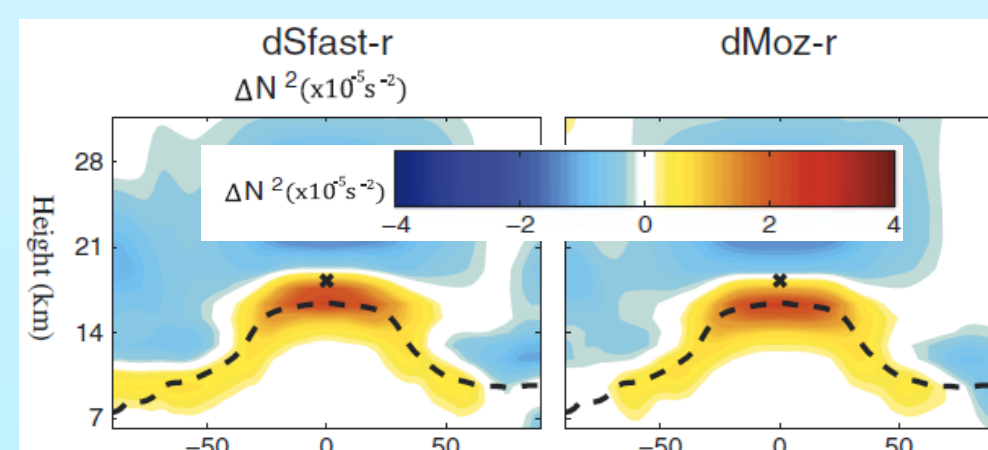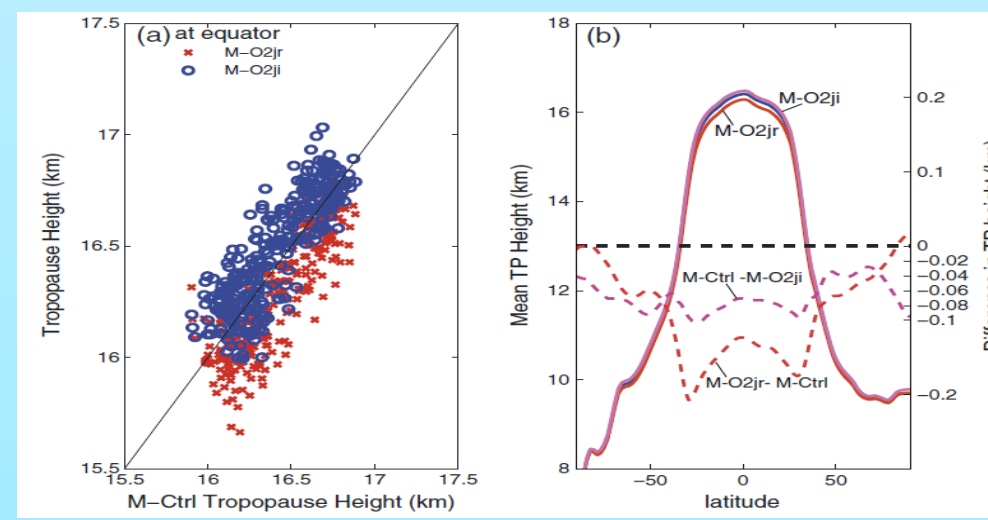
Fig. A3. Comparison of tropopause (tpp) heights for CAM5 MOZART-control vs. 30% cross-section reduction (M-O2jr) and 30% increase (M-O2ji). (a) Scatter plot shows monthly means in the tropics and (b) latitude-vs-tropopause height (km) shows differences. Note that differences for M-O2ji are plotted in the opposite sense (M-ctrl minus M-O2ji) to show similarity with M-O2jr.

Fig. A4. Mean decadal stratospheric polar temperature variances (°K^2) for SH and NH (60°-90°, >10 km), comparing the CAM4 Superfast control (-ctrl) and 30%-reduction (-O2jr) runs with those based on CAM5 MOZART.

Fast-J speeds up and morphs into Cloud-J and Solar-J

Fast-J has been implemented in CESM CAM5 and currently operates with the LLNL Superfast chemistry. At present LLNL and UCI are putting it on the trunk. At the request of WACCM, UCI developed a special data set for photolysis cross-sections to be used by WACCM. This version of Fast-J uses the same code but truncates all J-values to include only solar irradiance greater than 200 nm, where clouds and geo-engineered particles are likely to influence the chemistry and solar heating rates. WACCM will use it tabulated J-values for wavelengths <200 nm which are necessary to calculate chemistry above 60 km (the effective upper limit of the standard Fast-J version.

Fast-J is a critical element in the coupling of gas-phase chemistry, aerosols, clouds, and even geo-engineering through solar radiation management. For example, most all of the volatile organic compounds (VOCs) are destroyed primarily by photolysis and thus an accurate, interactive J-value code like Fast-J is needed (**Fig. B1**). The photochemistry of these VOCs is important in generating secondary organic aerosols (SOAs), which are an important climate driver (both direct radiative and indirect cloud effects).

Acceleration of Fast-J core computations. At UCI, working with computer scientists, the performance optimization of the *Fast-J* code tested the speedup capabilities that would be possible with CPU/GPU combinations. The primary computational cost of Fast-J is first the solution of a large block tri-diagonal matrix (4x4 x 200) for each column atmosphere for each wavelength (module blk_slv), and second the generation of 4x4 block matrices at each level and wavelength based on expansion of the scattering phase function in Associated Legendre Polynomials (module gen_id). A single instance of the tri-diagonal solver does not have enough parallelism to effectively utilize the GPU hardware, even when solving for all wavelengths at the same time. The solution we investigated was to solve the system for multiple air columns in parallel. Execution on a high-end Intel Core i7 processor was used as a baseline to derive the speedup factors for an NVIDIA Tesla C2070 GPU. Fast-J core operations (gen_id and blk_slv) were re-implemented in C with CUDA constructs to utilize the GPU. Speedups of at least 9x were obtained by our implementation on the Tesla C2070 when a large number of air columns are solved in parallel (**Table B1**). Future plans include simplifying the calculations, reducing the register dependences, load balancing among stream multiprocessors, generating launch configurations with warp scheduling, balancing and eliminate instruction pipelines stalls. We believe using CUDA the speedups of 18X may then be achievable. Currently a single column atmosphere calculation of J-values would likely involve 18 wavelengths by 4 different cloud profiles (72) and thus these speedup factors will require grouping a 10x10 cluster of column atmospheres in a single J-value calculation.

Cloud-J has completed independent tests in the UCI CTM and will now be implemented in CAM5 and WACCM. The Fast-J core code is nearly identical to that in Cloud-J and so implementation should be straightforward. Cloud-J allows the user (CAM5 or WACCM) to specify the cloud properties and fraction in each layer and then its method of overlap with other clouds in other layers. Cloud-J then offers 7 different approximations and one exact method (not operationally practical) to calculate the mean J-values in the column atmosphere.

The Cloud-J options are outlined in Table B2 and a sample result of several approximations is shown in Figure B2 for the J-value of NO_2. Note that clear-sky (ignoring clouds) has the same magnitude of error, but opposite sign, as average-clouds (smearing the clouds uniformly across each layer, effectively assuming cloud fraction equals 1). The use of four quadrature atmospheres is quite accurate as is the calculation of the direct beam and then inverting to get effective cloud layers (in a single column atmosphere). A common approximation is to reduce the cloud optical depth by the cloud fraction to the 3/2 power and then do average clouds. This method (#3 in the figure) is OK for this example, but accumulates much larger errors when one performs this test over a the full range of cloud distributions in the tropics (an example with 640 different cloud fields is not shown here).

PhotosyntheticallyActive Radiation. Fast-J is being modified to include a PAR action spectrum [Mccree, 1972] and to save the angular distribution of PAR incident on the surface. Accurate simulation of the total and direct-beam vs. diffuse PAR is needed for modeling ecosystem growth, carbon stocks, VOC emissions and many other aspects of terrestrial ecosystems. The effects of aerosols, particularly those of large volcanoes or geo-engineered stratospheric aerosols, have global impacts through changing the diffuse:direct ratio. Fast-J is one of the few solar radiation codes implemented with CAM5 that can accurately calculate this effect. Many solar radiative transfer codes, like RRTMG-SW, use a 2-stream approximation in which scattered light can only travel at a 55° zenith angle, whereas with Fast-J's 8-stream code, scattered light is resolved at 4 zenith angles (21°, 48°, 71°, 86°). The 2-stream methods must make further approximations by reducing the optical depth (OD) of forward-scattering clouds and aerosols and thus can err in under-representing the diffuse PAR. **Table B3** summarizes the PAR calculated by Cloud-J for a simple case study.

Solar-J will extend the Fast-J wavelength bands into the solar infrared (0.85 to ~5 µm) to allow for calculation of short-wave heating rates that are internally consistent with the aerosol and cloud fields used in the chemistry model (becoming Solar-J). As a quick demonstration of what Solar-J is capable of, we consider an atmosphere with a moderate stratospheric sulfate layer, cirrus clouds, mixed-phase clouds, biomass buring plumes, dust layers and a stratus deck in **Table B3** and **Figure B3**. The optical depth and single scattering albedo in each model layer are plotted, along with the heating rate. Note that the stratospheric sulfate layer enhances the heating rate through ozone absorption of the scattered light. Fast-J is not yet Solar-J, and so the heating rates include absorption by only ozone and aerosols over the wavelengths 187 to 850 nm. The water vapor bands in the O_3 Chappuis region (690-860 nm) are not included. The stratospheric sulfate layer corresponds to recent, large volcanic eruptions. The extension of Fst-J into the solar IR is not trivial, but several efforts, including RRTM and LLNL-work have looked at reducing the number of wavelengths needed so that the number of full-scattering calls by Fast-J would only double the cost. Unlike Cloud-J and PAR, this remains a multi-year project.

Fig. B1. VOC and related species photolysis loss frequencies (/day) as a function of altitude (km). The complex structure with altitude is due to a combination of increasing UV-radiation with altitude and Sterm-Volmer pressure dependences on quantum yields. We assume that the noon-time J's (tropical atmosphere, albedo=0.10, SZA=15°) apply for only 8 hours. Equivalent values for OH loss are shown with the species name in the legend and assume a noontime OH density of 6x10⁶ cm⁻³. Asterisks denote species with photolysis loss larger than or comparable to OH loss. VOC abbreviations are: MGlyoxal = methyl glyoxal; PropAld = propionaldehyde ; GlyAld = glycol aldehyde; MEKeto = methylethyl ketone; MeVK = methylvinyl ketone; ActAld = acetaldehyde; MeAcr = methacrolein; PAN = peroxyacetyl nitrate; C3H6O = acetone.

Table B1. Speedup factors of GPU/CPU vs. CPU

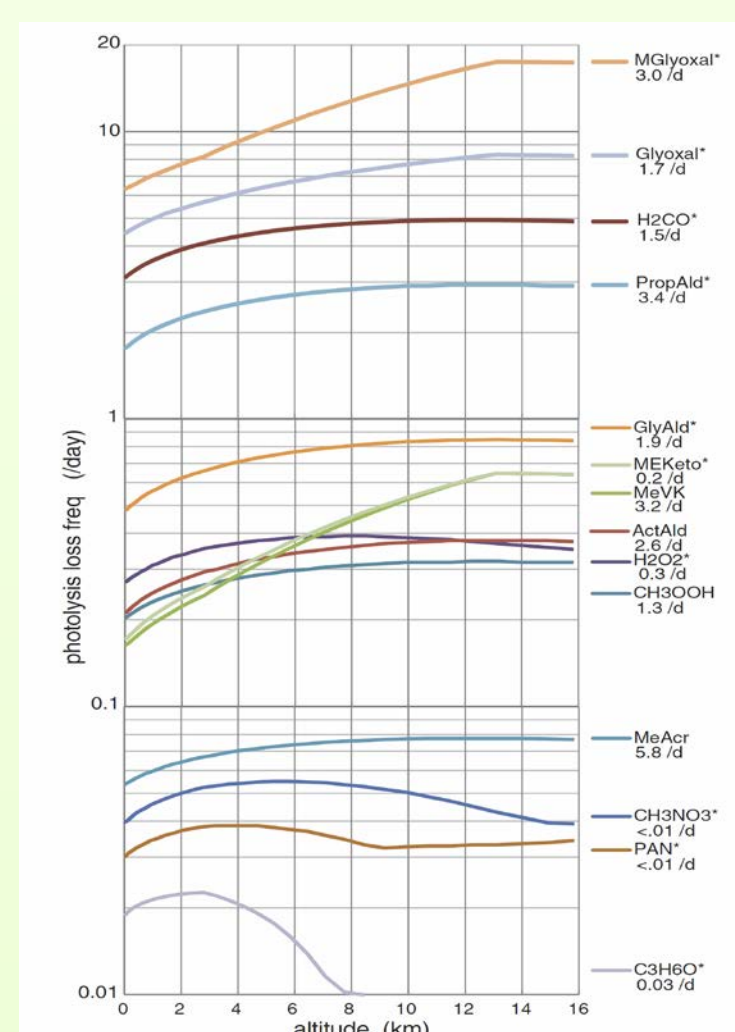| n (# columns)	gen_id speedup	blk_slv speedup
4032	9.3	10.7
5376	10.3	11.8
6720	10.6	12.7
7168	10.7	12.2

Fig. B2. J-values (/sec) for NO_2 calculated for a single grid box (UCI CTM 00H 1 Jan 2005, T42, J=32 & I=4) with a range of clouds from cumulus (1-9 km, small cloud fraction, OD ~20 per layer) to cirrus (11-14 km, large cloud fraction, OD ~ 0.4). The max-ran overlap model has 10 ICAs. The true answer is the average over the ICAs (#8, <ICAs>). The 4-point quadrature atmospheres (#7, <QCAs>) and the single ICA-equivalent cloud OD (#4) give similar results with pressure-weighted bias errors of <1%, but the clear sky (#1) and average cloud cover (#2, <cld>) have mean bias errors of -19% and +17%, respectively; pseudo-random approximation (#3, CF3/2) has +2.7% bias.
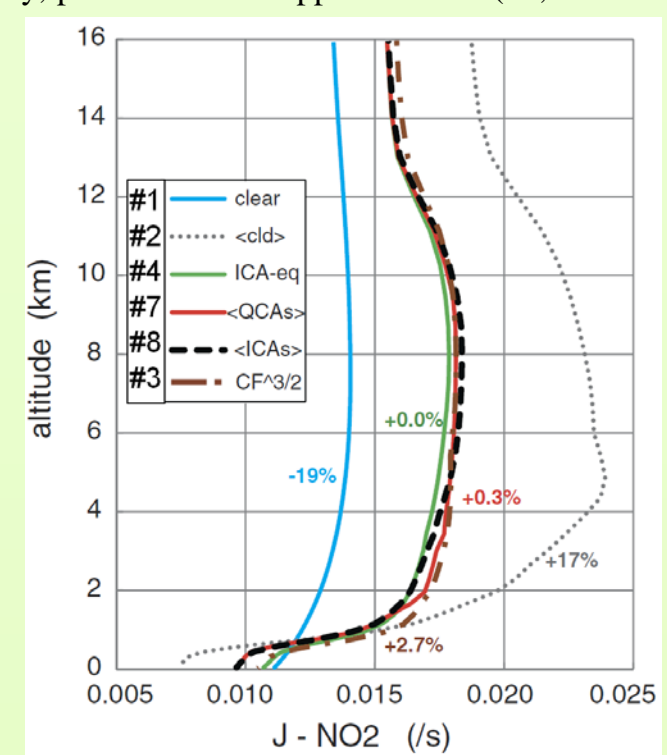
Table B2. Cloud-J options for sub-grid clouds

1	Clear sky J's
2	Average cloud cover
3	Cloud-Fraction**3/2, then avg cld cover
4	Average Direct Solar beam over all ICAs, inverted to get cloud OD in each layer
5	Random selection of ICA's from all
6	Quadrature QCAs, d4 (mid-pts of each Q-bin)
7	Quadrature QCAs, d4 (avg cld in each Q-bin)
8	All ICAs (up to 20,000)

Notes: Cloud-J is currently run with 3 groups of maximally overlapped clouds (0 – 1500m; 1500m to last liquid water cloud; all ice clouds), each of which is randomly overlapped with the other two.

Table B3. Sample Atmosphere - PAR & Solar-J

z(km)	type	OD	SSA
21	strat. sulf.	0.05	1.00
8-12	cirrus cld.	0.14	1.00
6-8	mixed cld.	0.04	1.00
7	biomass-burn	0.11	0.74
6	dust layer	0.06	0.95
0-2	water cld	5.0	1.00

surface albedo	0.10
solar zenith angle	13.6°
incident solar (<850 nm)	805 W/m²
reflected diffuse	298 W/m²
absorbed in atmosphere	87 W/m²
absorbed at surface	420 W/m²
PAR direct	0.3 µE/m²s
PAR diffuse	1265 µE/m²s

Notes: Typical tropical atmosphere. Optical Depth (OD) and Single Scattering Albedo (SSA) calculated by Fast-J at 600 nm.

Fig. B3. Fast-J/Solar-J sample atmosphere showing (i) aerosol & cloud optical depth in each layer, (ii) single scattering albedo (including O_3 absorption and Rayleigh scattering), and (iii) solar heating rates. Plotted symbols denote atmospheric layers. See Table B3 for summary of aerosol and cloud properties. Calculations are for a standard tropical atmosphere and ozone profile with solar zenith angle of 13.6°. Solar heating rates include only O_3 and aerosol absorption from 187-850 nm.

aerosol/cloud optical depth   single scattering albedo   heating rate (K/day)